Supplementary Methods:

Whole exome sequencing and analysis: Whole exome libraries were generated for DNA from Family 1 individuals II.7, III.5, and III.7 using the Nimblegen SeqCap EZ Human Exome library v2.0 kit (Roche Applied Science, Indianapolis, IN). Paired-end 50 bp sequencing was performed using a HiSeq2000 sequencing system (Illumina, San Diego, CA) according to the manufacturer's protocol. Sequence alignment and variant calling was performed against the reference human genome (UCSC hg18) using the Genome Analysis Toolkit (GATK version 1.0.5336, www.broadinstitute.org). PCR duplicates were removed prior to variant calling using Picard software (version 1.25, http://picard.sourceforge.net). Given autosomal dominant inheritance, sequence data were sorted for non-synonymous, heterozygous variants shared amongst the three affected patients. Variants identified in known databases (1000 genomes, dbSNP, and NHBLI Exome Variant Server) were excluded. After filtering, 14 single nucleotide variants and 2 indels remained for consideration (one indel was determined to be an exome artifact and was excluded). All Family 1 members collected (II.1, II.2, II.3, II.4, II.5, II.6, II.7, II.8, III.1, III.2, III.3, III.4, III.5, III.6, III.7, III.8, III.9, III.10, IV.1, IV.2) were subsequently Sanger sequenced to confirm variants and to check for segregation with disease. Following Sanger sequencing, only 1 novel variant remained: chr20: 10627741 in *JAG1*.

In Family 2, a whole-exome sequence library was generated from DNA from a single affected individual (II:5), with coding regions captured with a SureSelect Target Enrichment System and sequencing on a HiSeq system (Illumina) with 76 bp paired-end reads. Duplicate reads were assigned using Picard (v.1.46), with alignment using the Genome Analysis Toolkit (GATK, v.1.0.5777) and single-nucleotide variants called with GATK and SAMtools (v.0.1.16), and indels called with GATK and Dindel (v.1.01).

Genotyping and Haplotype Analysis: To ascertain whether the *JAG1* variant in Family 1 arose *de novo* in individual II.7, individuals II.6, II.7, II.8, III.5, III.7, and IV. 2 were genotyped on the Illumina NeuroChip array (1) which contains 486,137 SNPs, approximately 25,000 of which are custom variants linked to neurodegeneration. A disease haplotype was inferred in a 2-Mb region spanning the *JAG1* variant from chr20:9627479 (rs6077577) to chr20:11625510 (rs79628175). This region contains 372 NeuroChip variants. There are 42 informative SNPs based on comparison of II.6 and II.7 with their affected children (III.5, III.7) and grandchild (IV.2). Genomic positions are based on GRCh37/hg19.

Structural modeling: Tandem EGF-like repeats form linear solenoid domains common in the extracellular segments of cell surface proteins. EGF-like repeats each contain six cysteine residues which form three disulfide bridges, establishing a tertiary structure comprising a two-stranded β-sheet followed by a loop to a second, shorter two-stranded β-sheet (2). For structural modeling, the sequences of JAG1 EGF-like repeats 9-11 (residues 524 to 665) were manually aligned to the sequences of EGF-like repeats 3-5 of the canonical Notch ligand DLL1 (Supplementary Figure 1). The 27-residue extension around JAG1 EGF-like repeat 10 was aligned using either the UniProt (3) disulfide annotations or an alternative assignment that minimizes the number of insertions. The structural models were generated based on DLL1 (PDB ID 4XBM), using the structure of EGF-like repeats 3-5, manually repositioning repeat 5 relative to repeat 4 to match the canonical relative orientation between repeats as observed between repeats 3 and 4.

Western blot and cell surface biotinylation analyses: HEK293T (ATCC) and MN-1 (mouse motor neuron-neuroblastoma fusion cell line) cells were cultured in Dulbecco's modified Eagle's

medium (DMEM) supplemented with 10% (v/v) fetal calf serum, 100 U/ml penicillin, and 100 µg/ml streptomycin at 37°C with 6% CO_2. Cells were transfected with pFLAG-JAG1^{WT} (a gift of Minoru Tada), pFLAG-JAG1^{Ser577Arg} and pFLAG-JAG1^{Ser650Pro} (generated using the Q5 Site-Directed Mutagenesis Kit; New England Biolabs), pFLAG-JAG1^{Arg184His} (a gift of Minoru Tada), and pRK5M-ADAM17-Myc (a gift from Rik Derynck; Addgene, plasmid 31714) constructs, using Lipofectamine LTX (ThermoFisher). For analyses of whole cell lysates, cells were lysed at 24-48 hr post-transfection in RIPA buffer (Sigma) supplemented with protease inhibitors (Sigma) and sonicated. Cell surface biotinylation analyses were performed as in prior studies (4). Endo H (New England Biolabs) and PNGase F (New England Biolabs) digests were performed according to the manufacturer's instructions. Protein lysates were resolved on 4-15% TGX gels (Bio-Rad) and transferred to PVDF membranes (ThermoFisher). Primary antibodies used were monoclonal rabbit anti-FLAG (1:1000; Cell Signaling Technology, #2368), monoclonal rabbit anti-JAG1 (1:1000; Cell Signaling Technology, #2620), monoclonal rabbit anti-Myc Tag (1:1000; Cell Signaling Technology, #2272), monoclonal rabbit anti-β-actin (1:1000; Cell Signaling Technology, #4970) followed by a donkey anti-rabbit-HRP-conjugated secondary antibody (1:200,000; GE Healthcare). Membranes were developed using SuperSignal West Femto Maximum Sensitivity Substrate (ThermoFisher) and imaged using an ImageQuant LAS 4000 system (GE Healthcare). Densitometric analyses were performed using ImageJ (NIH) and Prism (v.8.1.2; GraphPad) software.

Immunocytochemistry: COS-7 cells (ATCC) were co-transfected with JAG1-FLAG and mApple-Sec61b-C1 (a gift from Jennifer Lippincott-Schwartz; Addgene, #90993) plasmids, as described above, and then replated onto poly-L-ornithine-coated coverslips after four hours. At 24 h post-transfection, cells were blocked for 30 min at 4°C in 0.1% bovine serum albumin (BSA) in

0.1 M phosphate-buffered saline (PBS; pH 7.4), and then incubated for 1 h at 4°C in the same solution containing an antibody raised against residues 32 to 296 of the JAG1 extracellular domain (1:40, polyclonal goat anti-JAG1; R&D Systems, AF1277). Cells were then fixed in 4% paraformaldehyde for 15 minutes at room temperature, permeabilized in PBS containing 0.3% Triton X-100, and blocked in 10% BSA in PBS. The cells were then incubated overnight at 4°C in a monoclonal mouse anti-FLAG (1:500; Sigma, F1804) primary antibody diluted in 3% BSA in PBS. Following rinsing, cells were incubated for 45 min at room temperature in Alexa 488-conjugated donkey anti-mouse and Alexa 647-conjugated donkey anti-goat secondary antibodies (1:1000; ThermoFisher). Coverslips were then rinsed, mounted in Prolong Diamond with DAPI (ThermoFisher), and imaged using a Zeiss LSM 800 Airyscan confocal microscope.

Generation of Jag1^{S577R} *knock-in mice:* Mice expressing the p.Ser577Arg mutation in the endogenous mouse *Jag1* gene were generated on the C57BL/6J strain (The Jackson Laboratory, Stock No. 000664) using CRISPR/Cas9 gene editing. The mutant allele was generated by substituting the serine codon at position 577 (AGC) with an arginine codon (AGA). A silent mutation at Val580 (GTG to GTC) was also introduced to eliminate a PAM site and prevent Cas9 re-cutting of targeted alleles. Three correctly targeted mutant founders (of 10 generated) were bred to C57BL/6J mice to demonstrate germline transmission. Experiments in the present study were performed on the strain designated JR29807. The approved allele description is C57BL/6J-*Jag1*^{em2Lutzy}/J. Following backcrossing to the C57BL/6J strain for three generations, heterozygous *Jag1*$^{S577R/+}$ males and females were intercrossed. Timed matings were performed according to (5). Genotyping was performed by amplifying a 430-bp fragment of the *Jag1* gene (forward primer: 5’ - TTT CTG TCC ACT TGG GAG TCT - 3’; reverse primer: 5’- AAT ACA TCT GCT CCC CCA AG - 3’), followed by digestion with the PvuII-HF restriction enzyme (New England

Biolabs). The nucleotide change generating the p.Ser577Arg mutation (AGC to AGA) removes a PvuII restriction site within the amplicon, resulting in a lack of sensitivity of the mutant allele to PvuII digest (see Supplementary Figure 4A-B). Despite extensive efforts, we have been unable to obtain living E8 *Jag1*$^{S577R/S577R}$ embryos for histological assessments of the cause(s) of lethality in these mice. We have obtained several dead *Jag1*$^{S577R/S577R}$ embryos at E8.5, however these have not proven informative due to rapid decomposition. Given that E8 represents a relatively early stage of embryonic development (e.g. prior to neural tube closure), exact determination of the cause(s) of lethality will require detailed further investigation. All procedures and experiments were approved by the Johns Hopkins University Animal Care and Use Committee and carried out in compliance with the National Institute of Health guidelines for the care and use of laboratory animals. The generation and establishment of the CRISPR/Cas9 genome edited strain JR29807 was carried out using procedures approved by The Jackson Laboratory Animal Care and Use Committee.

Motor behavior assessments: Assessments of motor behavior were performed on mixed gender cohorts of *Jag1*$^{S577R/+}$ mice and WT littermates (16-20 months of age) using the inverted grid test and accelerating rotarod assay. All testing was performed in the evening by experimenters blinded to animal genotype. The inverted grid test (also known as the four limb wire grid holding test) (6) was performed by placing mice upright on a wire mesh grid situated 40 cm above soft matting. The grid was then inverted and the latency to fall measured using a stopwatch. Testing consisted of three trials per day, with intertrial intervals of 3-5 min, performed one day per week for three weeks. Body weight was measured immediately prior to the first trial on each day, and did not differ between the WT and *Jag1*$^{S577R/+}$ cohorts (Supplementary Figure 4C). Holding impulse (N s), which represents the force exerted by the inverted mouse to oppose the gravitational force

associated with its body mass (6), was calculated by multiplying body weight (g) x 0.00980665 (N/g) x average latency to fall (s). The accelerating rotarod assay was performed by placing up to four littermate mice on the rotarod apparatus (Rotamex, Columbus Instruments) rotating at a constant speed of 4 rpm. Once all mice were facing the rear of the apparatus, the rotation speed of the rod was accelerated over 5 minutes to 40 rpm at intervals of 0.6 rpm every 5 seconds. Latency to fall was recorded automatically for each trial. Testing consisted of three trials per day, with intertrial intervals of 3-5 min, performed one day per week for three weeks.

Peripheral nerve electrophysiology: Compound muscle action potentials (CMAPs) were recorded from the plantar muscles of the hind paw following stimulation of the sciatic nerve, using an Evidence 3102eco EMG system (Schreiber & Tholen Medizintechnik, Germany). Briefly, mice (at 19-23 months of age) were anesthetized using 2-3% isoflurane, a recording electrode inserted into the left plantar muscles, and the ipsilateral sciatic nerve stimulated using short (<0.2 ms duration), supramaximal electrical impulses at a proximal (sciatic notch) and a distal (ankle) site (7). The area and latency of recorded responses were determined using Neuro-MEP software (Neurosoft). All recordings and analyses were performed by experimenters blinded to animal genotype.

Transmission electron microscopy (TEM): Mice at 19-23 months of age were anaesthetized deeply with isoflurane, transcardially perfused with 3% glutaraldehyde/4% paraformaldehyde (PFA), and then postfixed overnight in the same fixative. Following rinsing in 0.1 M Sorensen's buffer, the recurrent laryngeal nerve was dissected free, postfixed using 2% osmium tetroxide, and dehydrated through a graded series of ethanol dilutions. The nerves were then embedded in propylene oxide and EMbed 812 plastic (Electron Microscopy Sciences) and placed in an oven to

harden into capsule form. Semi-thin sections (1 μm) were cut on an ultramicrotome and multiple sections were placed on Superfrost slides, dried, stained with toluidine blue, and viewed by light microscopy. Thin sections for TEM were then cut at 60-90 nm, placed on Formvar grids and viewed using a Zeiss Libra 120 transmission electron microscope. Reconstructed images of the entire recurrent laryngeal nerve were generated in Adobe Photoshop using series of overlapping images. G-ratio was calculated by dividing the diameter of an individual axon with the diameter of its myelin sheath. Diameters (*d*) were derived from measurements of axon and myelin sheath circumference (*c*; $d = c/\pi$).

Immunohistochemistry: Mice at 19-23 months of age were anaesthetized deeply with isoflurane, perfused transcardially with 2% PFA, and then postfixed overnight with 2% PFA. The posterior cricoarytenoid muscle (the vocal fold abductor muscle) was dissected free, teased into small myofiber bundles, and labelled using monoclonal mouse anti-neurofilament M and H (1:1000; BioLegend, 837904, clone SMI312) and monoclonal rabbit anti-synaptophysin (1:500; ThermoFisher, MA5-14532, clone SP11) antibodies, followed by Alexa Fluor 488-conjugated goat anti-mouse IgG, Fcγ subclass specific (1:200; Jackson ImmunoResearch Laboratories,) and Alexa Fluor 647-conjugated goat anti-rabbit IgG (1:200; Jackson ImmunoResearch Laboratories, 111-605-144) secondary antibodies together with Alexa Fluor 555-conjugated α-Bungarotoxin (1:500; ThermoFisher). Images were obtained using a Zeiss LSM 800 Airyscan confocal microscope.

Mutation Mapping: Our description of the mutations follows HGVS nomenclature guidelines (http://varnomen.hgvs.org/) and is based on sequence from RefSeq Transcript NM_000214. The JAG1 protein sequences were aligned using the Clustal Omega sequence alignment tool (8). The

Alagille syndrome-causing missense mutations shown in Figure 2B are described in (9-16).

Supplementary Table 1: Phenotypic characteristics of affected subjects

	Patient	Age at time of exam (yr)	Sex	Age of onset (yr)	First symptom	Vocal fold paresis	Limb weakness		Sensory loss	Reflexes
							Proximal	Distal		
Family 1	II.7	73	M	childhood	stridor	mild	none	mild	mild	areflexic
	III.5	44	F	birth	stridor	severe, requiring tracheostomy	none	mild	mild	areflexic
	III.7	49	F	birth	stridor	moderate	none	mild	mild	areflexic
	IV.2	19	F	birth	stridor	severe, requiring tracheostomy	none	mild	mild	areflexic
Family 2	II.3	43	M	childhood	stridor	severe, requiring tracheostomy	none	none	normal, poor circulation	present
	II.1	59	M	childhood	stridor	right palsy, reduced mobility on left	none	none	poor circulation	hyporeflexic ankle jerks
	II.2	54	F	childhood	stridor	left palsy, reduced mobility right	none	none	normal	present
	III.2	33	F	childhood	stridor	severe, requiring tracheostomy	mild triceps weakness	none	normal	areflexic in lower extremities

Supplementary Table 2: Nerve conduction studies of affected patients.

	Family 1						Family 2					
	III.5 age 31		**III.7** age 48		**IV.2** age 18		**II.2** age 54		**II.1** age 59		normal values	
	Amplitude	Velocity	Amplitude	Velocity	Amplitude	Velocity	Amplitude	Velocity	Amplitude	Velocity	Amplitude	Velocity
SENSORY	µV	m/s	µV	m/s	µV	m/s	µV	m/s	µV	m/s	µV	m/s
radial	ND	ND	6.1	50	8.7	57.1	18		9.0		≥15	≥50
median	ND	ND	ND	ND	16.6	54.5	10.0	40	5.0	61	≥10	≥50
sural	7	55	8.1	40	7.6	45.2	21	42	14	47	≥7	≥50
MOTOR	mV	m/s	mV	m/s	mV	m/s	mV	m/s	mV	m/s	mV	m/s
peroneal	1.8	49	2.2	40.8	NR	NR	3	48	2.4	46	≥2.0	≥41
median	8.2	60	10.9	57.9	3.2	49.4	10	55	12.8	61	≥4.0	≥49
tibial	ND	ND	ND	ND	1.7	51	ND	ND	ND	ND	≥6.0	≥49
EMG	Myokymia-like discharges		TA: chronic denervation		VL: fibrillations and large motor units TA: large motor units		TA: occasional polyphasis units Larynx: large complex potentials, chronic denervation		TA: occasional polyphasis units Larynx: large complex potentials, chronic denervation			

Supplementary Table 3: CMT2-associated variants are predicted to be damaging in multiple *in silico* predictors of functional importance or conservation.

In Silico Predictor	**p.Ser577Arg**	**p.Ser650Pro**
PolyPhen-2	probably damaging, 0.996	probably damaging, 0.979
Panther	probably damaging, 798	probably damaging, 455
SNPs&GO	disease, RI: 5, probability: 0.744	disease, RI: 7, probability: 0.836
SNAP2	effect, score 75, expected accuracy85%	effect, score 60, expected accuracy %80
Mutation Taster	disease causing, score 110	disease causing, score 74
Mutation Assessor	medium, score 2.44	medium, score 2.735
FATHMM	Damaging, -2.32	damaging, -1.6
SIFT	damaging	damaging
CADD	24.2	27.7

Supplementary Table 4: Mendelian ratios of progeny from heterozygous intercrosses of *Jag1*^{S577R} knock-in mice.

Age	Genotype	No. observed	No. expected*	χ^2 analysis (p value)
E8.5-12.5	*WT*	23	23	<0.0001
	Jag1$^{S577R/+}$	47	46	
	Jag1 $^{S577R/ S577R}$	1	23	
Postnatal	*WT*	52	52	<0.0001
	Jag1 $^{S577R/+}$	93	104	
	Jag1 $^{S577R/S577R}$	0	52	

***** assumes that WT mice were observed at the expected frequency and a 1:2:1 segregation ratio

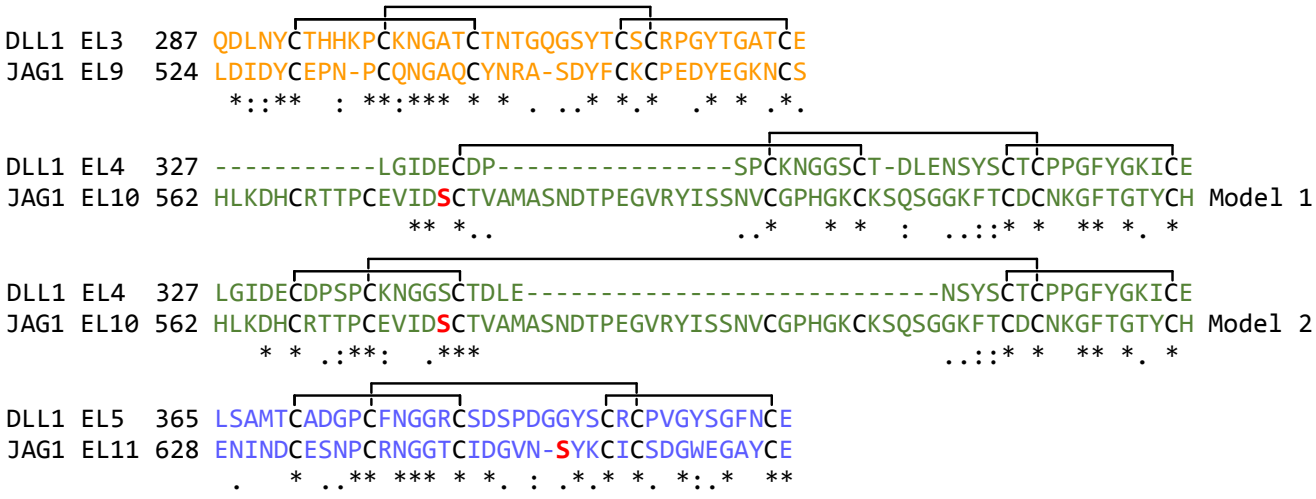

Supplementary Figure 1. Sequence alignment of DLL1 EGF-like repeats 3-5 and JAG1 EGF-like repeats 9-11 used for structural modeling. The JAG1 EGF-like repeats are aligned according to UniProt disulfide annotations in Model 1, and using an alternative cysteine alignment that minimizes the number of insertions in Model 2. Color coding is consistent with Figure 2C-D.

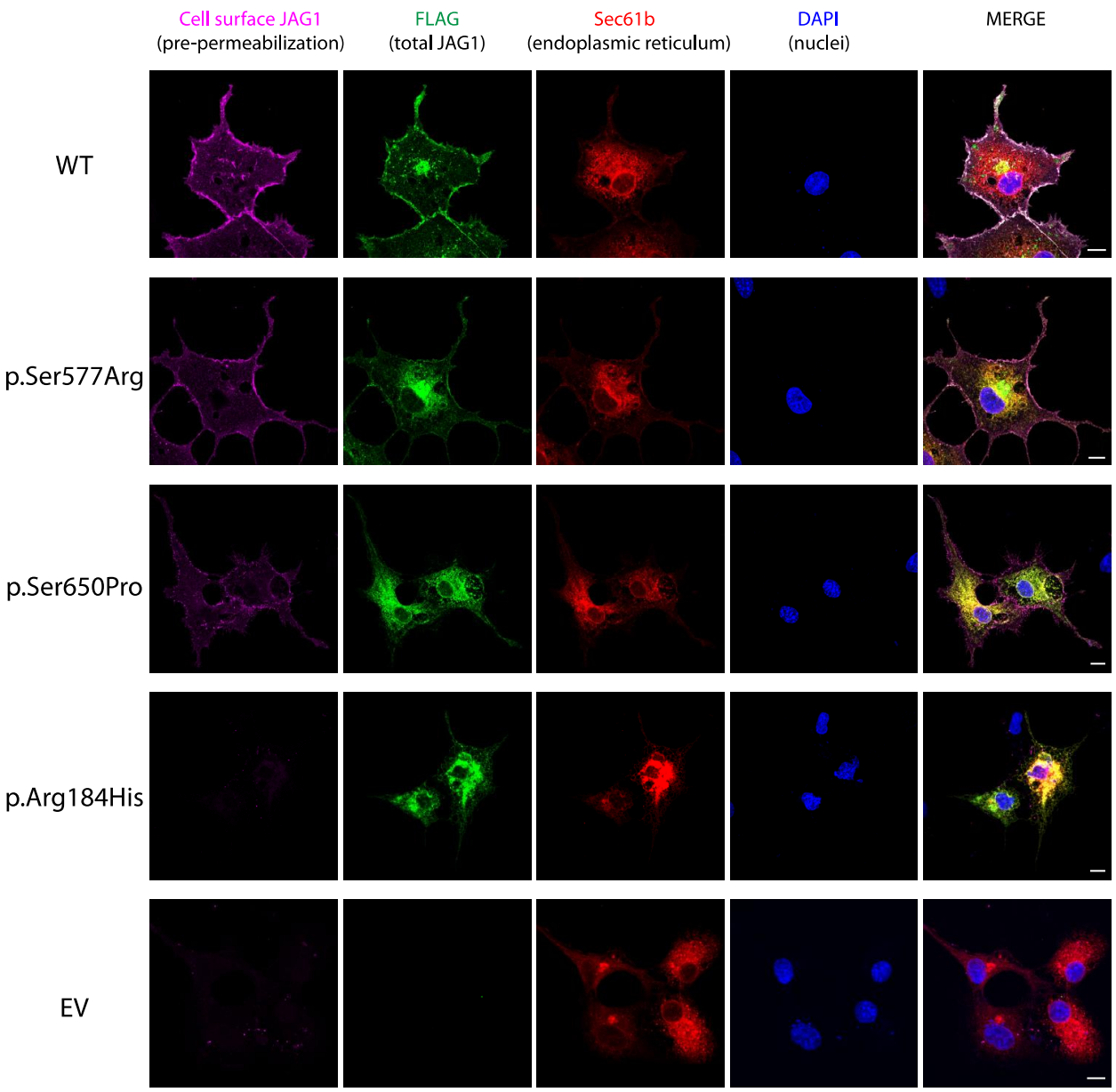

Supplementary Figure 2. Individual maximum intensity projection confocal images comprising the merged images shown in Figure 3A. Scale bars, 10 µm.

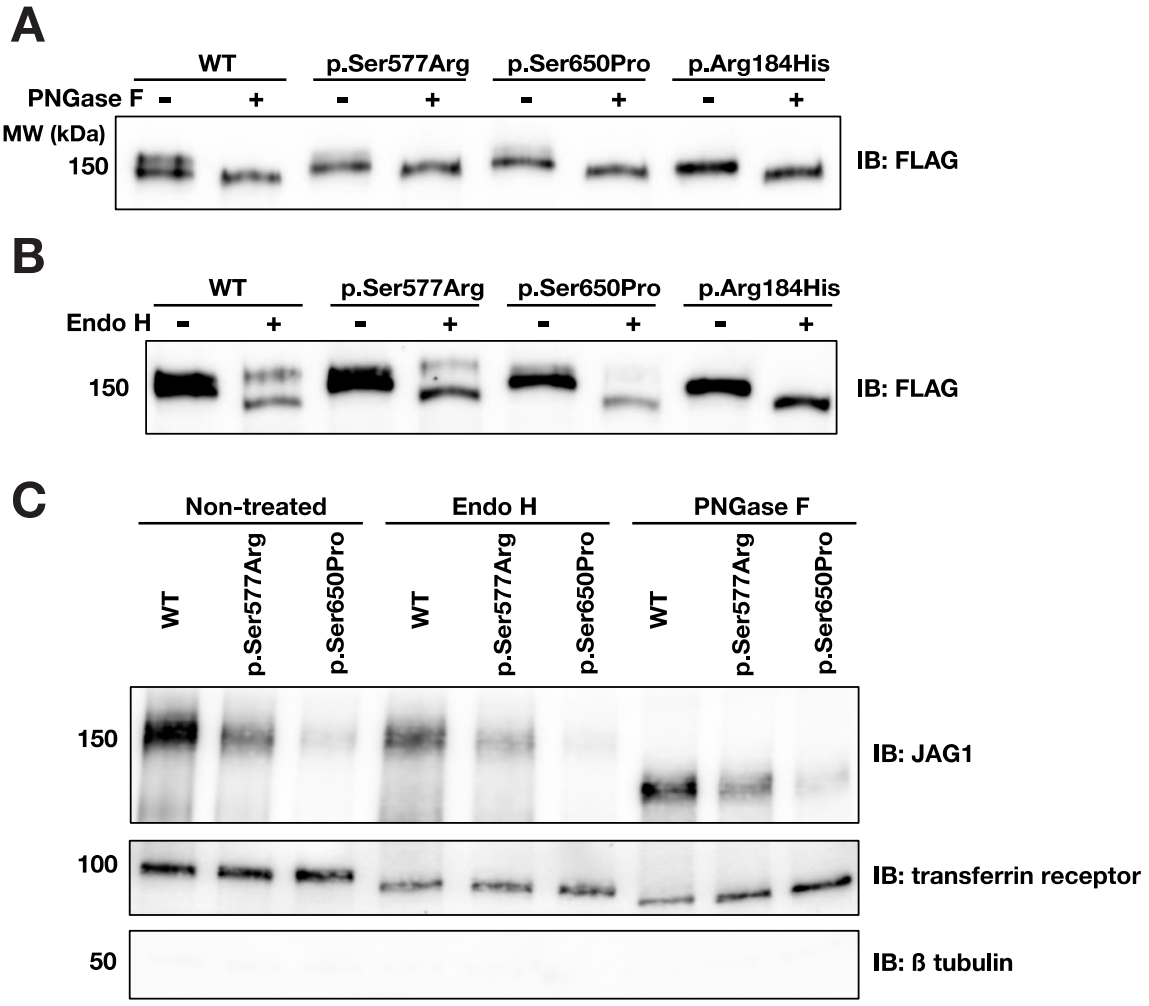

Supplementary Figure 3. Deglycosylation treatments of WT and mutant JAG1. (A, B) Western blot analysis of whole cell lysates from transfected MN-1 cells following deglycosylation using PNGase F **(**A**)** and Endo H **(**B**)**. Note that the higher molecular weight band is sensitive to treatment with PNGase F (which removes all *N*-linked glycans), but not Endo H (which removes only simple glycans), indicating that it represents a complex glycosylated form of JAG1, as described previously (17, 18). **(C)** Deglycosylation treatments of cell surface (biotinylated) proteins from transfected HEK293T cells (see Figure 3F-G) indicate that only the complex glycosylated forms of $JAG1^{WT}$ and the CMT2-associated mutants are present at the plasma membrane.

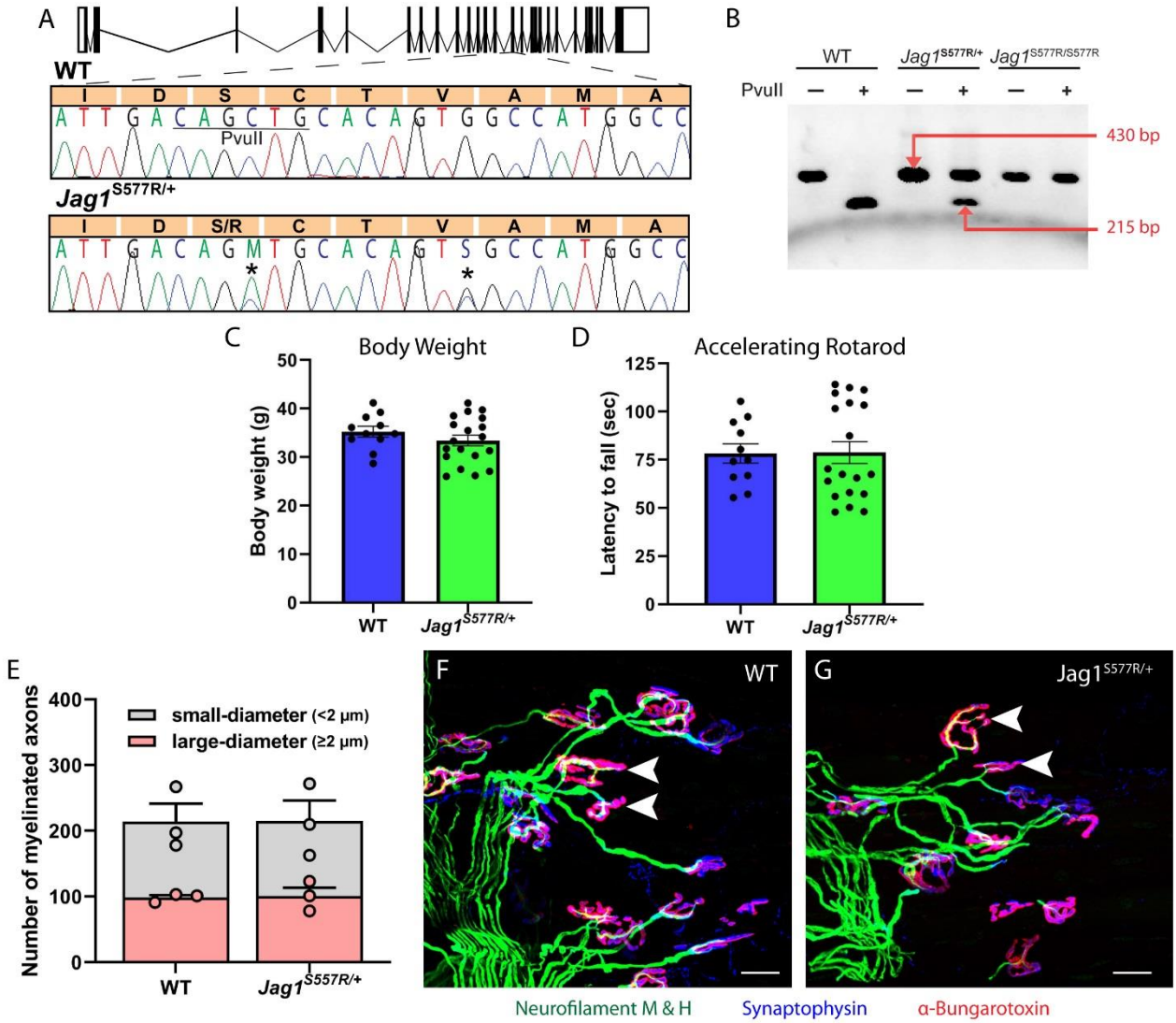

Supplementary Figure 4. Generation, genotyping, and characterization of *Jag1*^{S577R} knock-in mice. (A) The mouse *Jag1* exon structure is shown. Exon 14 was targeted using CRISPR/Cas9 to generate a novel knock-in mouse model expressing the *Jag1*^{S577R} mutation in the endogenous mouse gene. Sanger sequencing traces show successful generation of the mutant allele containing both the *Jag1*^{S577R} mutation and a silent mutation introduced to eliminate a PAM site and prevent Cas9 re-cutting of targeted alleles. **(B)** The nucleotide change generating the p.Ser577Arg mutation removes a PvuII restriction site, enabled genotyping of the mutant allele via its insensitivity to PvuII digestion. **(C)** Body weights of *Jag1*$^{S577R/+}$ and WT littermate mice on which

motor behavioral assessments were performed. **(D)** *Jag1*$^{S577R/+}$ mice exhibited normal performance on the accelerating rotarod assay (n=11 for WT, n=19 for *Jag1*$^{S577R/+}$). (**E**) Myelinated axon number in the recurrent laryngeal nerve of *Jag1*$^{S577R/+}$ and WT littermate mice (n=3 for WT, n=3 for *Jag1*$^{S577R/+}$). (**F-G**) Absence of neuromuscular junction denervation in the posterior cricoarytenoid muscle of WT (F) and *Jag1*$^{S577R/+}$ (G) littermate mice. Arrowheads indicate representative, fully innervated neuromuscular junctions. Scale bars, 20 μm.

```
H. sapiens      MRSPRTRGRSGRPLSLLLALLCALRAKVCGASGQFELEILSMQNVNGELQNGNCCGGARN   60
M. musculus     MRSPRTRGRPGRPLSLLLALLCALRAKVCGASGQFELEILSMQNVNGELQNGNCCGGVRN   60
                ********* ************************************************.**

H. sapiens      PGDRKCTRDECDTYFKVCLKEYQSRVTAGGPCSFGSGSTPVIGGNTFNLKASRGNDRNRI   120
M. musculus     PGDRKCTRDECDTYFKVCLKEYQSRVTAGGPCSFGSGSTPVIGGNTFNLKASRGNDRNRI   120
                ************************************************************

H. sapiens      VLPFSFAWPRSYTLLVEAWDSSNDTVQPDSIIEKASHSGMINPSRQWQTLKQNTGVAHFE   180
M. musculus     VLPFSFAWPRSYTLLVEAWDSSNDTIQPDSIIEKASHSGMINPSRQWQTLKQNTGIAHFE   180
                *************************:******************************:****

H. sapiens      YQIRVTCDDYYYGFGCNKFCRPRDDFFGHYACDQNGNKTCMEGWMGPECNRAICRQGCSP   240
M. musculus     YQIRVTCDDHYYGFGCNKFCRPRDDFFGHYACDQNGNKTCMEGWMGPDCNKAICRQGCSP   240
                *********:**************************************:**:**********

H. sapiens      KHGSCKLPGDCRCQYGWQGLYCDKCIPHPGCVHGICNEPWQCLCETNWGGQLCDKDLNYC   300
M. musculus     KHGSCKLPGDCRCQYGWQGLYCDKCIPHPGCVHGTCNEPWQCLCETNWGGQLCDKDLNYC   300
                ********************************** ************************

H. sapiens      GTHQPCLNGGTCSNTGPDKYQCSCPEGYSGPNCEIAEHACLSDPCHNRGSCKETSLGFEC   360
M. musculus     GTHQPCLNRGTCSNTGPDKYQCSCPEGYSGPNCEIAEHACLSDPCHNRGSCKETSSGFEC   360
                ******** ***************************************************** ****

H. sapiens      ECSPGWTGPTCSTNIDDCSPNNCSHGGTCQDLVNGFKCVCPPQWTGKTCQLDANECEAKP   420
M. musculus     ECSPGWTGPTCSTNIDDCSPNNCSHGGTCQDLVNGFKCVCPPQWTGKTCQLDANECEAKP   420
                ************************************************************

H. sapiens      CVNAKSCKNLIASYYCDCLPGWMGQNCDININDCLGQCQNDASCRDLVNGYRCICPPGYA   480
M. musculus     CVNARSCKNLIASYYCDCLPGWMGQNCDININDCLGQCQNDASCRDLVNGYRCICPPGYA   480
                ****:********************************************************

H. sapiens      GDHCERDIDECASNPCLNGGHCQNEINRFQCLCPTGFSGNLCQLDIDYCEPNPCQNGAQC   540
M. musculus     GDHCERDIDECASNPCLNGGHCQNEINRFQCLCPTGFSGNLCQLDIDYCEPNPCQNGAQC   540
                ************************************************************

H. sapiens      YNRASDYFCKCPEDYEGKNCSHLKDHCRTTPCEVIDSCTVAMASNDTPEGVRYISSNVCG   600
M. musculus     YNRASDYFCKCPEDYEGKNCSHLKDHCRTTTCEVIDSCTVAMASNDTPEGVRYISSNVCG   600
                ***************************** ************************************

H. sapiens      PHGKCKSQSGGKFTCDCNKGFTGTYCHENINDCESNPCRNGGTCIDGVNSYKCICSDGWE   660
M. musculus     PHGKCKSQSGGKFTCDCNKGFTGTYCHENINDCESNPCKNGGTCIDGVNSYKCICSDGWE   660
                ****************************************:*********************

H. sapiens      GAYCETNINDCSQNPCHNGGTCRDLVNDFYCDCKNGWKGKTCHSRDSQCDEATCNNGGTC   720
M. musculus     GAHCENNINDCSQNPCHYGGTCRDLVNDFYCDCKNGWKGKTCHSRDSQCDEATCNNGGTC   720
                **:**.*********** ****************************************

H. sapiens      YDEGDAFKCMCPGGWEGTTCNIARNSSCLPNPCHNGGTCVVNGESFTCVCKEGWEGPICA   780
M. musculus     YDEVDTFKCMCPGGWEGTTCNIARNSSCLPNPCHNGGTCVVNGDSFTCVCKEGWEGPICT   780
                *** *:**************************************:***************:

H. sapiens      QNTNDCSPHPCYNSGTCVDGDNWYRCECAPGFAGPDCRININECQSSPCAFGATCVDEIN   840
M. musculus     QNTNDCSPHPCYNSGTCVDGDNWYRCECAPGFAGPDCRININECQSSPCAFGATCVDEIN   840
                ************************************************************

H. sapiens      GYRCVCPPGHSGAKCQEVSGRPCITMGSVIPDGAKWDDDCNTCQCLNGRIACSKVWCGPR   900
M. musculus     GYQCICPPGHSGAKCHEVSGRSCITMGRVILDGAKWDDDCNTCQCLNGRVACSKVWCGPR   900
                **:*:**********:***** ***** ** ******************:***********

H. sapiens      PCLLHKGHSECPSGQSCIPILDDQCFVHPCTGVGECRSSSLQPVKTKCTSDSYYQDNCAN   960
M. musculus     PCRLHKSHNECPSGQSCIPVLDDQCFVRPCTGVGECRSSSLQPVKTKCTSDSYYQDNCAN   960
                ** ***.*.**********:********:*********************************

H. sapiens      ITFTFNKEMMSPGLTTEHICSELRNLNILKNVSAEYSIYIACEPSPSANNEIHVAISAED   1020
M. musculus     ITFTFNKEMMSPGLTTEHICSELRNLNILKNVSAEYSIYIACEPSLSANNEIHVAISAED   1020
                ********************************************* **************

H. sapiens      IRDDGNPIKEITDKIIDLVSKRDGNSSLIAAVAEVRVQRRPLKNRTDFLVPLLSSVLTVA   1080
M. musculus     IRDDGNPVKEITDKIIDLVSKRDGNSSLIAAVAEVRVQRRPLKNRTDFLVPLLSSVLTVA   1080
                *******:****************************************************

H. sapiens      WICCLVTAFYWCLRKRRKPGSHTHSASEDNTTNNVREQLNQIKNPIEKHGANTVPIKDYE   1140
M. musculus     WVCCLVTAFYWCVRKRRKPSSHTHSAPEDNTTNNVREQLNQIKNPIEKHGANTVPIKDYE   1140
                *:**********:*******.****** ********************************

H. sapiens      NKNSKMSKIRTHNSEVEEDDMDKHQQKARFAKQPAYTLVDREEKPPNGTPTKHPNWTNKQ   1200
M. musculus     NKNSKMSKIRTHNSEVEEDDMDKHQQKVRFAKQPVYTLVDREEKAPSGTPTKHPNWTNKQ   1200
                **************************.******.********* *.**************

H. sapiens      DNRDLESAQSLNRMEYIV   1218
M. musculus     DNRDLESAQSLNRMEYIV   1218
                ******************
```

Supplementary Figure 5: Clustal Omega alignment of human and mouse JAG1 amino acid sequence demonstrates a 96.6% identity with conservation of both CMT2-associated variants. There are 87 serine residues in the human JAG1 protein (shown in red), none are mutated in Alagille syndrome.

Clinical features of JAG1-associated axonal neuropathy:

Family 1:

Family 1, III.7: The patient was first noted to have stridor at birth and has experienced stridor with exertion since that time. At 49 years old, otorhinolaryngology examination revealed bilateral vocal fold motion impairment (left>right) with decreased abduction bilaterally. Motor exam showed mild weakness of first dorsal interosseous and abductor digiti minimi muscles. Sensory examination showed reduced pinprick sensation and temperature sensation in the distal legs, reduced vibration at the toes, and normal proprioception. She was globally areflexic. Gait was normal. She has mild scoliosis with convexity to the left. At age 55, she subjectively notes progressive hand weakness. She has no history of liver, cardiac, or renal disease and receives regular medical care.

Family 1, IV.2: At birth, the patient had audible stridor and required oxygen. She had a tracheostomy placed at 1 month of age for management of vocal fold paresis (Fig. 1e). Hypotonia was noted during the first few months of life and walking was delayed; occurring at 21 months of age. She had a thoracic level 2-12 spinal fusion at age 9 and thoracic 12-lumbar 4 fusion at age 13 for scoliosis (Fig. 1e). No vertebral body malformation was noted. She has lifelong mild *pes cavus* (Fig. 1e). At age 19, her motor exam showed full proximal strength with bilateral weakness in first dorsal interosseous, tibialis anterior and toe extensor muscles (all MRC grade 4/5). Sensory exam revealed reduced pinprick and temperature sensation in the distal extremities, mildly reduced vibratory sensation to the knee, and normal proprioception. She was diffusely areflexic. Her gait was normal except for mildly impaired heel walking.

Family 1, III.5: The patient was first noted to have stridor at birth. She was evaluated at age 15 at Mayo Clinic for stridor with limited exertion. At age 17, she was noted to have a 2 mm airway and underwent a vocal fold tie-back procedure. Repeat ENT examination at age 44 showed bilateral vocal fold motion impairment (left>right) with abductor paresis. She had two episodes of pneumonia with respiratory insufficiency including an ICU stay. At age 45, following one of these episodes of pneumonia, a tracheostomy was placed, which she keeps capped during the day. Audiology examinations showed mild hearing loss. She has noted lifelong *pes cavus*. At age 44, motor exam showed normal proximal upper extremity strength and mild weakness bilaterally in flexor digitorum indicis, abductor pollicus brevis, and abductor digiti minimi muscles (all

MRC grade 4/5). Sensory exam showed mildly reduced vibratory, pinprick, and temperature sensation distally in legs and normal proprioceptive. She is areflexic. Gait exam revealed difficulty walking on her heels. At age 50, she notes gradual worsening of hand strength. She receives regular medical care and has no history of liver, cardiac, of kidney disease.

Family 1, II.7: The patient reported a history of stridor with exertion since childhood, but was only diagnosed with vocal fold paresis during evaluation at NIH in his early 60s. ENT exam at that time showed left vocal fold abduction paresis. He notes increased difficulty with breathing in cold weather. He has lifelong *pes cavus*. At age 73, motor exam showed atrophy in intrinsic hand muscles and distal leg muscles. He had normal proximal strength with mild weakness bilaterally in flexor digitorum indicis, abductor pollicus brevis, abductor digiti minimi, tibialis anterior, toe extensor, and toe flexor muscles (all MRC grade 4/5). Sensory exam showed decreased vibratory, pinprick, and temperature sensation in all distal extremities with reduced proprioception only to fine movements at the great toe. He was areflexic. His gait exam revealed some difficulty walking on his heels and slight ataxia with tandem walk. In his late 70s, he was diagnosed with coronary artery disease with complicating myocardial infarction. He has also had a lacunar stroke in his basal ganglia with minimal residual deficits. There is a family history of coronary artery disease in other family members without the JAG1 variant.

Family 2:

Family 2, III.2: The patient has always had a slightly stridorous voice, becomes breathless on exertion, and has found it difficult to shout. She also had a history of kyphoscoliosis, migraine, and night sweats. At age 20 she was referred to neurology for frequent non-painful muscle twitches. Her power appeared normal other than mild triceps muscle weakness. Upper limb reflexes were normal and lower limb reflexes absent. Bilateral *pes cavus* was noted. Sensation was normal, as were cranial nerves and examination of the fundus. At 41 years, breathing difficulties increased and she required a tracheostomy due to bilateral vocal fold paralysis. She also developed some symptoms of dysphagia.

Family 2, II.3: The patient has a long history of breathing difficulties that were variously diagnosed as asthma and chronic bronchitis. He has a history of kyphoscoliosis since childhood and was also said to have finger clubbing. He was diagnosed at age 43 years with bilateral vocal fold paralysis and required a tracheostomy. At that time, he also complained of continuous

muscle “activity” and gave a history of night sweats and was referred to a neurologist for evaluation. On examination he had bilateral finger clubbing and mild bilateral pitting edema of both ankles. Hands and feet appeared cold and had changes of poor circulation with poorly healing leg ulcers. He had a tremor affecting his hands. Extensive muscle fasciculations were noted in the periorbital region and in the limbs. Power was documented as normal and deep tendon reflexes were present. *Pes cavus* was also noted. A needle muscle biopsy of the left quadriceps showed mild group atrophy especially affecting type 2 fibers. There were occasional central nuclei and several regenerating myofibres. This was interpreted to represent chronic denervation. Creatine kinase was just above the upper limit of normal 310 IU/L (upper limit normal range 195).

Family 2, II.2: The patient was evaluated at age 54. She recalled that as a child she became breathless on exertion and she was diagnosed with vocal fold paralysis at the age of 41 years. She also complained of twitches around her right eye from the age of 12 years. She described periodic spontaneous extension of the hallux on both feet which started in childhood. She had type 2 diabetes mellitus (diet controlled) and a hiatal hernia. Examination of her hands revealed tremor with polyminimyoclonus in the fingers. Manual dexterity was normal. She had reduced arm swing on the right when walking with abnormal posturing of the hand. Power and reflexes appeared normal. Laryngoscopy showed paralysis of the left vocal fold which was immobile but not in the midline position. There was also reduced mobility of the right vocal fold. EMG of the laryngeal muscles showed features of chronic denervation. MRI brain scan was normal.

Family 2, II.1: The patient was evaluated at the age of 59 years. As a child, he noted that he was never able to shout or sing. He had an inspiratory stridor. He had a history of abdominal bloating, red hands and feet, and periodic swelling of his feet. He described occasional night sweats, vivid dreams, nightmares, and possible urinary frequency. He also reported a past history of “dizzy spells” approximately 10 years prior to the evaluation, which had since resolved. On examination he had purplish-blue hands and feet, associated with mild edema and trophic changes in his feet. Further investigations of dysautonomia were recommended to the patient, but he did not attend any follow-up evaluations. Power was normal and ankle jerks were hypoactive. He had a fine pseudotremor of his hands with arrhythmic jerks of the fingers elicited by sensitive stimulus or stretch consistent with polyminimyoclonus. There was bilateral *pes cavus* with retraction of the hallux. Laryngoscopy revealed right vocal fold paralysis and reduced movement of the left vocal

fold. EMG of the laryngeal muscles showed large complex potentials that were felt to be consistent with chronic denervation (Supplementary Table 2).

References in this Supplementary Material:

1. Blauwendraat C, et al. NeuroChip, an updated version of the NeuroX genotyping platform to rapidly screen for variants associated with neurological diseases. *Neurobiol Aging*. 2017;57:247 e249-247 e213.

2. Cordle J, et al. A conserved face of the Jagged/Serrate DSL domain is involved in Notch trans-activation and cis-inhibition. *Nat Struct Mol Biol*. 2008;15:849-857.

3. The UniProt Consortium. UniProt: the universal protein knowledgebase. *Nucl Acids Res*. 2017;45(D1):D158-D169.

4. Landouré G, et al. Mutations in TRPV4 cause Charcot-Marie-Tooth disease type 2C. *Nat Genet*. 2010;42:170-174.

5. Mader SL, Libal NL, Pritchell-Corning K, Yang R, Murphy SJ. Refining timed pregnancies in two strains of genetically engineered mice. *Lab Anim*. 2009;38:305-310.

6. Carlson CG, et al. A simple protocol for assessing inter-trial and inter-examiner reliability for two noninvasive measures of limb muscle strength. *J Neurosci Methods*. 2010;186:226-230.

7. Tallon C, Russell KA, Sakhalkar S, Andrapallayal N, Farah MH. Length-dependent axo-terminal degeneration at the neuromuscular synapses of type II muscle in SOD1 mice. *Neuroscience*. 2016;312:179-189.

8. Sievers F, et al. Fast, scalable generation of high-quality protein multiple sequence alignments using Clustal Omega. *Mol Syst Biol*. 2011;7:539.

9. Krantz ID, et al. Spectrum and frequency of jagged1 (JAG1) mutations in Alagille syndrome patients and their families. *Am J Hum Genet*. 1998;62:1361-1369.

10. Crosnier C, et al. Mutations in JAGGED1 gene are predominantly sporadic in Alagille syndrome. *Gastroenterology*. 1999;116:1141-1148.

11. Pilia G, et al. Jagged-1 mutation analysis in Italian Alagille syndrome patients. *Hum Mutat*. 1999;14:394-400.

12. Heritage ML, MacMillan JC, Colliton RP, Genin A, Spinner NB, Anderson GJ. Jagged1 (JAG1) mutation detection in an Australian Alagille syndrome population. *Hum Mutat*. 2000;16:408-416.

13. Colliton RP, Bason L, Lu FM, Piccoli DA, Krantz ID, Spinner NB. Mutation analysis of Jagged1 (JAG1) in Alagille syndrome patients. *Hum Mutat*. 2001;17:151-152.

14. Eldadah ZA, et al. Familial Tetralogy of Fallot caused by mutation in the jagged1 gene. *Hum Mol Genet*. 2001;10:163-169.

15. Röpke A, Kujat A, Graber M, Giannakudis J, Hansmann I. Identification of 36 novel Jagged1 (JAG1) mutations in patients with Alagille syndrome. *Hum Mutat*. 2003;21:100.

16. Warthen DM, et al. Jagged1 (JAG1) mutations in Alagille syndrome: increasing the mutation detection rate. *Hum Mutat*. 2006;27:436-443.

17. Morrissette JD, Colliton RP, Spinner NB. Defective intracellular transport and processing of JAG1 missense mutations in Alagille syndrome. *Hum Mol Genet*. 2001;10:405-413.

18. Tada M, Itoh S, Ishii-Watabe A, Suzuki T, Kawasaki N. Functional analysis of the Notch ligand Jagged1 missense mutant proteins underlying Alagille syndrome. *FEBS J*. 2012;279:2096-2107.